Available online at www.sciencedirect.com
ScienceDirect
Ceramics International 37 (2011) 1533–1536
CERAMICS INTERNATIONAL
www.elsevier.com/locate/ceramint

IR reflectance characterization of glass–ceramic films obtained by high pressure impregnation of SnO_2 nanopowders on float glass

T. Sequinel [a,*], S. Cava [b], J.O. Pimenta [c], S.A. Pianaro [c], S.M. Tebcherani [c], J.A. Varela [a]

[a] *Instituto de Química, UNESP, R. Francisco Degni, s/n, bairro Quitandinha, CEP 14800-900, Araraquara, SP, Brazil*
[b] *Universidade Federal de Pelotas, Rua Gomes Carneiro, 1 Centro, CEP 96010-610, Pelotas, RS, Brazil*
[c] *Universidade Estadual de Ponta Grossa, Av. General Carlos Cavalcanti, 4748, CEP 84030-900, Ponta Grossa, PR, Brazil*

Received 2 September 2010; received in revised form 19 November 2010; accepted 10 January 2011
Available online 3 February 2011

Abstract

Glass–ceramic thin films of tin dioxide on float glass surfaces were obtained using a method based on high pressures and temperatures below the glass transition temperature. SnO_2 thin films were confirmed using XRD, SEM and XRF techniques. These thin films were identified using IR reflectance due to a shift induced by Sn ion content of about ~100 cm^{-1} in the main maximum peak position which is typical of stretching vibration intensities of a $\nu_{Si-O-Si}$ bridging bonds, or a ν_{Si-O^-} nonbridging bonds.

Keywords: Nanostructures; Thin films; Glasses; Infrared spectroscopy

1. Introduction

The presence of a tin atom in the glass lattices produces several changes in their physicochemical properties [1–4]. In previous research differences in the chemical composition between the upper and bottom surfaces of float glass were detected using IR reflection spectra [5]. Despite numerous infrared studies devoted to amorphous SiO_2, considerable controversy exists concerning the origin of high-frequency absorption peaks between ~1000 and 1300 cm^{-1} [6–10].

Thin films are typically deposited on glass surfaces by electrostatic spray [11,12] or saline solution deposition techniques using the chemical effect of temperature [13,14], which result in films containing metal ions on the glass surface. Another way to change the properties of glasses is directly related to doping the composition of oxide mixtures prior to performing the glass processing [1,15].

In recent years a new way to impregnate nano-oxides on float glass surfaces using high pressures and temperatures below the glass transition has been developed [16]. After impregnation under high gas pressure, the metal oxides form a second phase on the film which may be amorphous or nanocrystalline, depending on factors such as the chemical composition of the glass, size and specific surface area of the metal oxide powders, gas pressure and the type of gas applied, as well as the temperature and time [17].

SnO_2 nanocrystals embedded in silica glass matrices of bulk dimensions are now an extensively researched for supply the advancing technology demands increasingly to smaller optical components [18]. SnO_2 also has the advantages of being extremely stable both chemically and mechanically [19] and of possessing a high refractive index (1.99 at 632 nm). All these qualities are necessary for the successful preparation of optical waveguides. Finally, the small particle size also has the advantage of preventing scattering losses in the planar waveguides [18].

The aim of the present work is to study supplementary information about the chemical and structural changes in thin films prepared by forced impregnation of ultrafine SnO_2 powders on the float glass surface [16]. Our focus is to clarify several observed physicochemical features which are related to this method of film formation. The most common techniques used for surface analysis have been employed such as: IR spectroscopy, low-angle X-ray diffraction and X-ray fluores-

* Corresponding author. Tel.: +55 16 8155 8613; fax: +55 16 3322 0015.
E-mail addresses: sequinel.t@iq.unesp.br (T. Sequinel), sergiocava@gmail.com (S. Cava), jupimenta_pr@hotmail.com (J.O. Pimenta), sap@uepg.br (S.A. Pianaro), sergiomt@uepg.br (S.M. Tebcherani), varela@iq.unesp.br (J.A. Varela).

0272-8842/$36.00
doi:10.1016/j.ceramint.2011.01.013

cence spectroscopy. Scanning electron microscopy (SEM) was performed in order to detail the influence of time on film growth.

2. Experimental

Commercial float glasses (Saint-Gobain) were used in these experiments, and the glass sheets were cut into 20 mm × 20 mm × 2 mm samples. The weight composition of glass samples used in this study was SiO_2 (57.9%), CaO (25.9%), Na_2O (11.5%), MgO (3.2%), Al_2O_3 (0.8%), and K_2O (0.70%).

SnO_2 powders used to obtain thin films were supplied by Itajara Minérios Ltda [20] with the following characteristics: 3.7 nm of crystallite size calculated by Scherrer's method; 4.2 nm of mean diameter calculated by the BET method; and 0.9 μm of average particle size estimated from SEM micrographs.

Thin films were processed at low temperatures (below the glass transition) and high gas pressure (1.72 MPa) [16]. The main points of this process are: (a) deposition of metal oxide powders on the glass surface; (b) application of cold gas under high pressure into a hermetically closed heating chamber; (c) infiltration of powder onto the glass-plate surface and (d) heating to a temperature below the glass transition temperature (∼550 °C) as a function of time.

Several preliminary tests helped to determine some parameters for the process developed here, resulting in the use of a temperature of 485 °C and a gas pressure of 1.72 MPa applied for 32 h.

The composition of glass–ceramic thin films obtained by the gas pressure impregnation of powders was characterized by X-ray fluorescence using a Shimadzu EDX 700 spectrometer. Film crystallization was verified by low-angle X-ray diffraction using a Shimadzu XRD6000 diffractometer with CuKα radiation (λ = 1.5406 Å) in the 2θ range of 20–80° with 0.02°/min scans. The surface morphology was characterized by SEM (Shimadzu SSX550).

IR reflectance spectra were registered using an IR spectrophotometer (Nicolet 4700) and employing a halogen lamp light source. Data were obtained with a resolution of 1 cm^{-1} per step.

3. Results and discussion

First, the glass–ceramic films obtained by gas pressure impregnation were characterized by X-ray fluorescence to determine the film composition.

The main constituents of the glass substrates and SnO_2 glass–ceramic films are listed in Table 1.

Table 1
Chemical composition of glass substrate and SnO_2 glass–ceramic film obtained by pressure impregnation.

	SnO_2	SiO_2	CaO	NaO_2	MgO	Al_2O_3	K_2O
Glass		57.9	25.9	11.5	3.2	0.8	0.7
Glass + film	5.6	57.4	25.4	7.0	3.1	0.8	0.7

Analyzing the X-ray fluorescence data, a change is observed in just one component in relation to the initial composition of the glass substrate. The volatility of sodium atoms on the glass surface [21] results in an ion exchange where the NaO_2 was replaced by SnO_2, reaching about 5 wt% of tin dioxide in the glass composition.

Low-angle X-ray diffraction measurements were used to determine the purity and the crystallization of the glass–ceramic film. Fig. 1 shows the low-angle diffraction patterns of the glass–ceramic film obtained by gas pressure impregnation of SnO_2 powders on the glass surface.

The diffractogram presented in Fig. 1 shows a predominance of amorphous morphology from the glass substrate. A detailed analysis shows that, despite the low content (∼5.5%) of SnO_2 powders impregnated on the glass substrate, some peaks (301 and 321) were observed and assigned to the tetragonal rutile SnO_2 phase (JCPDS card 41-1445).

The glass–ceramic film morphology was visualized by SEM. Some SEM micrographics were superimposed to demonstrate the growth and formation of a tin dioxide film on the glass substrate surface as a function of time, varying from 0 to 32 h with constant temperature at 485 °C and a pressure of 1.72 MPa (Fig. 2).

An analysis of Fig. 2 shows that region (a – 0 h) is representative of a float glass substrate without the deposition of a SnO_2 film which is equivalent to the initial time of treatment. In the region (b – 8 h), some nucleation points can be visualized which are responsible for initializing the growth of the film. Starting from the nucleation points, a large growth of the film (c – 16 h) can be observed in the next steps. A small grain growth occurs in the region (d – 24 h) until a complete densification of the glass–ceramic film (e – 32 h) is finalized as representative cycles for the growth of this film.

This film process using high pressure favored the diffusion generated at the interface of the glass substrate with SnO_2 nanopowders and the deepness of the film was about 700 nm [17].

The presence of SnO_2 film on a glass surface was confirmed using an IR spectroscopy test. The tin concentration leads to

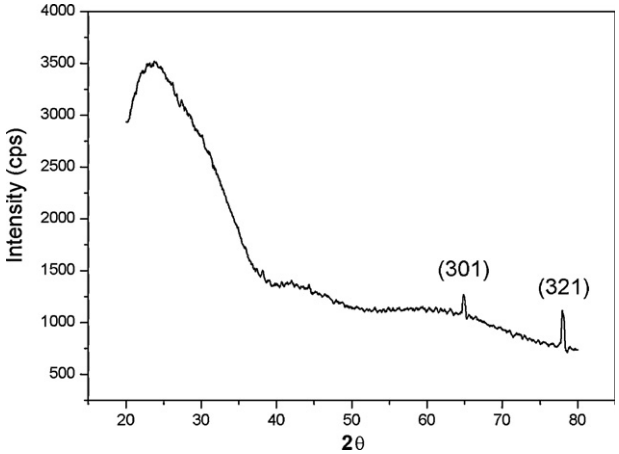

Fig. 1. Low-angle diffractogram of glass–ceramic film infiltrated onto float glass substrate.

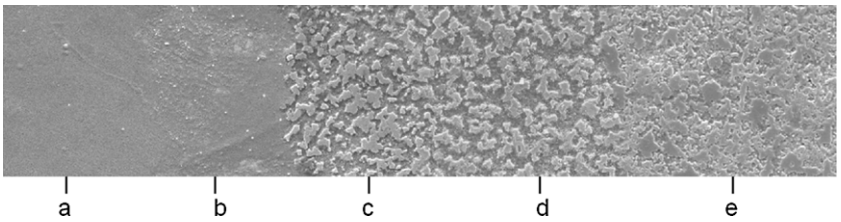

Fig. 2. Superimposed SEM micrographs of glass–ceramics films at 485 °C in different time: (a) 0 h (pure commercial float glass), (b) 8 h, (c) 16 h, (d) 24 h, (e) 32 h (homogeneous glass–ceramics thin film).

structural modifications in the glass which decreases the number of $\nu_{Si-O-Si}$ bridging bonds and increases the number of ν_{Si-O^-} nonbridging bonds [5]. Since SnO_2 film was deposited on only one side of the glass, this side was denoted as the top surface (with film). The other side (opposite the film) was denoted as the bottom surface; the IR spectra presented in Fig. 3 shows a comparison between both the top and bottom surfaces in relation to the float glass (without film).

These spectra show a shift in the main maximum peaks typical of the stretching vibration intensities of the $\nu_{Si-O-Si}$ bridging bonds, and the ν_{Si-O^-} nonbridging bonds. The $\nu_{Si-O-Si}$ main maximum peak from the top surface (Fig. 3a – 1044 cm^{-1}) has been displaced about 100 cm^{-1} in relation to the float glass (Fig. 3c – 1144 cm^{-1}). For comparison, a similar shift occurs for the ν_{Si-O^-} nonbridging bonds wavelength between the float glass surface (Fig. 3c – 1081 cm^{-1}) and the top surface (Fig. 3a – 993 cm^{-1}) which results in a wavelength variation of about 88 cm^{-1}.

A change in the wavelength in the bottom surface is revealed (Fig. 3b) due to the impregnation of SnO_2 particles in the glass matrix which occurred due to the high pressure treatment used in the film synthesis.

The observed shift on the band peaking at 1100 cm^{-1} is attributed to the stretching vibration of Si–O–Si, shifted to the smaller energy side after SnO_2 film deposition. The redshift in silica, observed for SnO_2 film deposition, reflects the decrease in Si–O–Si bond angles [22], leading to densification of glass. These data strongly suggest a change in the glass structures resulting from the contact of SiO_2 surface.

The Sn ion content in the SnO_2 impregnated films is responsible for different spectra in relation to the float glass without a film. Previous researches [5] showed that just 1 wt% of a Sn ion is sufficient to displace the spectral position about 5–10 cm^{-1} for a SiO_2 matrix. In the present study, the SnO_2 film results in a 5 wt% of the glass surface components.

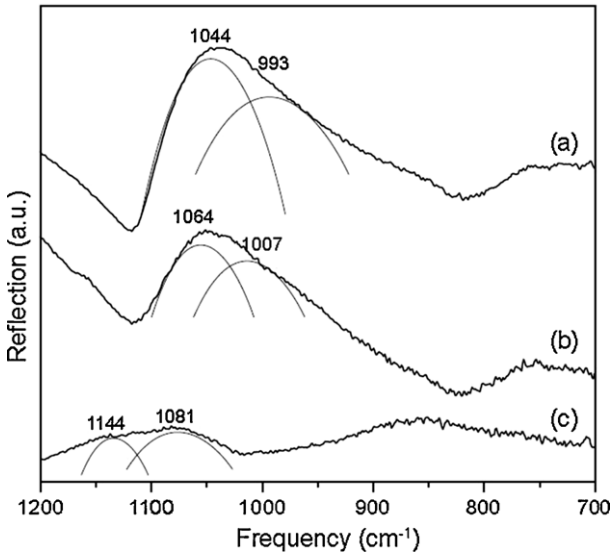

Fig. 3. IR reflection spectra of float glass: (a) top surface with film, (b) bottom surface opposite to film, (c) float glass without film.

4. Conclusions

Tin dioxide glass–ceramic films were obtained on a float glass surface using a pressure of 1.72 MPa and an annealing temperature at 485 °C. XRD, SEM and XRF results confirmed the efficiency of this methodology for the synthesis of glass–ceramic films. SnO_2 glass–ceramic films are identified by IR reflectance spectroscopy because the tin dioxide content in the glass surface results in a shift of about 100 cm^{-1} in the main maximum peak position which is typical of the stretching vibration intensities of the $\nu_{Si-O-Si}$ bridging bonds and 88 cm^{-1} for the ν_{Si-O^-} nonbridging bonds.

Acknowledgements

The authors gratefully acknowledge the financial support of the Brazilian financing agencies FAPESP, FINEP and CNPq.

References

[1] E.C. Ziemath, B.Z. Saggioro, J.S. Fossa, J. Non-Cryst. Solids 351 (52–54) (2005) 3870–3878.
[2] E.C. Ziemath, V.D. Araújo Jr., C.A. Escanhoela, J. Appl. Phys. 104 (5) (2008), 054912.
[3] M.H. Krohn, J.R. Hellmann, B. Mahieu, C.G. Pantano, J. Non-Cryst. Solids 351 (6–7) (2005) 455–465.
[4] F. Bent Julian, C. Hannon Alex, Diane Holland, Mustamam M.A. Karim, J. Non-Cryst. Solids 232–234 (1998) 300–308.
[5] O.A. Gladushko, A.G. Chesnokov, Glass Ceram. 62 (9) (2005) 308–309.
[6] E.I. Kamitsos, A.P. Patsis, G. Kordas, Phys. Rev. B 48 (17) (1993) 12499–12505.
[7] P. McMillan, Am. Mineral. 69 (7–8) (1984) 622–644.
[8] L. Stoch, M. Sroda, J. Mol. Struct. 511 (1999) 77–84.
[9] M.H. Modi, G.S. Lodha, M.K. Tiwari, S.K. Rai, C. Mukharjee, P. Magudapathy, K.G.M. Nair, R.V. Nandedkar, Nucl. Instrum. Methods Phys. Res. Sect. B 239 (4) (2005) 383–390.

[10] L.S. Roman, R. Valaski, C.D. Canestraro, E.C.S. Magalhães, C. Persson, R. Ahuja, E.F. da Silva, I. Pepe, A.F. da Silva, Appl. Surf. Sci. 252 (15) (2006) 5361–5364.
[11] H. Gómez-Pozos, A. Maldonado, M.L. Olvera, Mater. Lett. 61 (7) (2007) 1460–1464.
[12] K.S. Hwang, J.H. Jeong, Y.S. Jeon, K.O. Jeon, B.H. Kim, Ceram. Int. 33 (3) (2007) 505–507.
[13] X. Ma, A. Liu, H. Xu, G. Li, M. Hu, G. Wu, Mater. Res. Bull. 43 (8–9) (2008) 2272–2277.
[14] A.Y. Zhang, T. Suetsugu, K. Kadono, J. Non-Cryst. Solids 353 (1) (2007) 44–50.
[15] J.A. Johnson, J. Urquidi, D. Holland, C.E. Johnson, P.G. Appelyard, J. Non-Cryst. Solids 353 (44–46) (2007) 4084–4092.
[16] S. Cava, T. Sequinel, S.M. Tebcherani, M.D. Michel, S.R. Lazaro, S.A. Pianaro, J. Alloys Compd. 484 (2009) 877–881.
[17] S. Cava, T. Sequinel, S.M. Tebcherani, M.D. Michel, C.M. Lepienski, J.A. Varela, J. Non-Cryst. Solids 356 (2010) 215–219.
[18] T. Van Tran, S. Turrell, M. Eddafi, B. Capoen, M. Bouazaoui, P. Roussel, S. Berneschi, G. Righini, M. Ferrari, S.N.B. Bhaktha, O. Cristini, C. Kinowski, J. Mol. Struct. 976 (2010) 314–319.
[19] T. Toupance, O. Babot, B. Jousseaume, G. Villaca, Chem. Mater. 15 (2003) 4691.
[20] T. Sequinel, S. Cava, D. Berger, S.M. Tebcherani, S.A. Pianaro, S. Schmidt, Powder Technol. 196 (2009) 180–183.
[21] H.K. Jang, S.W. Whangbo, Y.K. Choi, K. Jeong, C.N. Whang, C.H. Wang, D.J. Choi, S. Lee, J. Non-Cryst. Solids 296 (3) (2001) 182–187.
[22] K. Kawamura, N. Sarukura, M. Hirano, H. Hosono, Appl. Phys. Lett. 78 (8) (2001) 1038–1040.